

Surface vibrations of diamond C(001)(2×1)

S. Thachepan, H. Okuyama, T. Aruga, and M. Nishijima

Department of Chemistry, Graduate School of Science, Kyoto University, Kyoto 606-8502, Japan

T. Ando

National Institute for Material Sciences (NIMS), 1-1 Namiki, Tsukuba, Ibaraki 305-0044, Japan

S. Bağcı and H. M. Tütüncü

Sakarya Üniversitesi, Fen-Edebiyat Fakültesi, Fizik Bölümü, Adapazarı, Turkey

G. P. Srivastava

School of Physics, University of Exeter, Stocker Road, Exeter EX4 4QL, United Kingdom

(Received 4 March 2003; published 17 July 2003)

Surface vibrations of diamond C(001)(2×1) have been studied by means of electron energy loss spectroscopy as well as first-principles theoretical calculations. Several vibrational modes are newly resolved. Outside the bulk phonon band, we observe a surface-derived mode at 172 meV, which is assigned as the dimer stretching mode as predicted by theoretical results. The other losses are in resonance with the bulk phonon band, and thus, they cannot be assigned as pure surface or bulk modes. The dispersions of the loss peaks are measured along the high-symmetry directions of the surface Brillouin zone, where we find nearly localized character of the vibrations along the surface.

DOI: 10.1103/PhysRevB.68.033310

PACS number(s): 68.35.Ja, 68.49.Uv, 79.20.Uv

The surface vibrational property is one of the most fundamental issues for surface physics since it is proximately related to the surface dynamical processes of, e.g., surface reconstruction and surface phase transitions. Surface phonons of crystalline materials have been vastly investigated by means of electron energy loss spectroscopy (EELS) and He atom scattering (HAS).¹

Diamond has attracted much attention from both experimentalists and theorists owing to its intrinsic properties such as a large band gap, high saturation carrier velocity, and high thermal conductivity. A number of experimental as well as theoretical studies, focused on the vibrational properties of diamond C(001)(2×1) surfaces, have been performed.²⁻⁸ Figure 1(a) shows the schematic structure of the C(001)(2×1) surface. The surface phonons of C(001)(2×1) were experimentally observed mainly using EELS.^{2,3,7,8} In previous studies, the C(001)(2×1) surface showed vibrational spectra with an intense loss centered at 92 meV and several losses ranging from 120 to 170 meV.^{7,8} Since the attainable resolutions were rather low, we believe there are still a number of unresolved structures.

The phonon energies of C(001)(2×1) were calculated at the $\bar{\Gamma}$ point of the surface Brillouin zone (SBZ).⁴⁻⁶ Since the C-C surface dimer bond is rehybridized to $\sim sp^2$ on C(001)(2×1), the dimer C-C stretching mode of C(001)(2×1) was predicted to be split from the bulk band.⁴⁻⁶

In this study, we investigate the vibrational modes of the diamond C(001)(2×1) surface by means of EELS as well as first-principles theoretical calculations. We detect several new losses and measure the surface phonon dispersions along the high-symmetry directions of the SBZ. The losses are assigned mainly by comparison with previous and present theoretical works.

The experiments were performed by using an ultrahigh-vacuum chamber equipped with a high-resolution electron spectrometer for EELS (LK-5000, LK Technologies, Inc.), an electron optics for low-energy electron diffraction (LEED), and a quadrupole mass spectrometer for gas analysis. The base pressure of the chamber was less than 1×10^{-10} Torr.

A B-doped diamond film was epitaxially grown on the (001) surface of synthesized single-crystalline diamond (1b type) using the microwave plasma-assisted chemical vapor deposition (CVD) method. The thickness of the CVD film was $\sim 20 \mu\text{m}$. The typical B concentration in the CVD diamond film was at the ppm level. The size of the substrate was $4 \times 4 \times 0.3 \text{ mm}^3$. The sample was mounted on a tantalum holder. The sample could be cooled to 90 K using a liquid nitrogen reservoir and heated to 1400 K by electron bombardment from the back side. The sample temperature

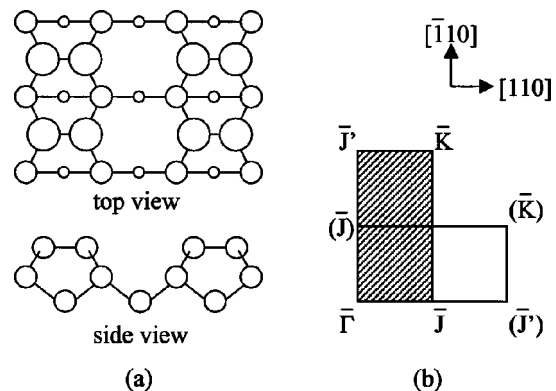


FIG. 1. (a) Structural model of the diamond C(001)(2×1) surface (top and side views). (b) The corresponding surface Brillouin zone (SBZ).

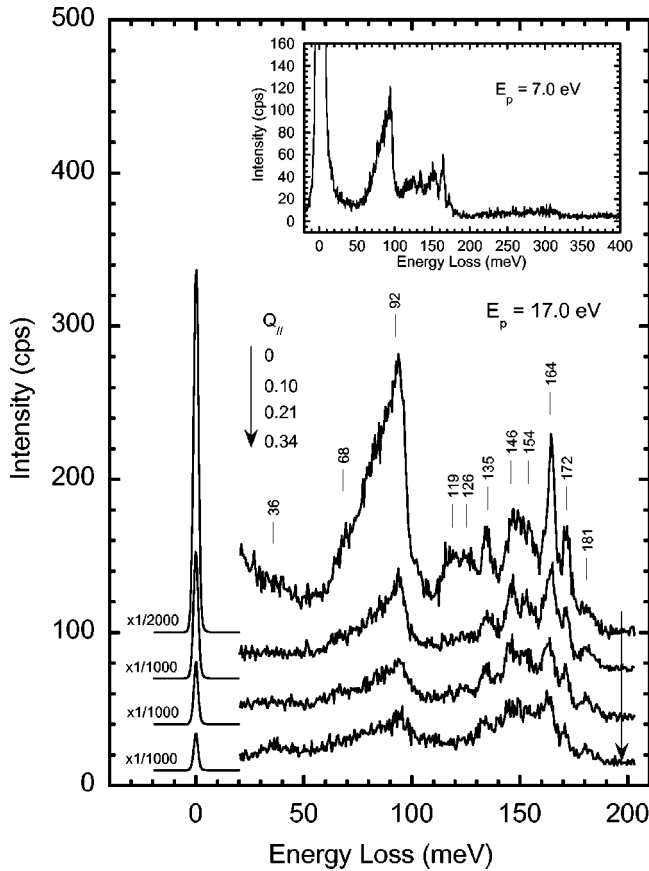


FIG. 2. The EELS spectra of the clean C(001)(2×1) surface at 90 K as a function of the momentum transfer, Q_{\parallel} , with $E_p = 17.0$ eV and $\theta_i = 60^\circ$. The emission angles (θ_e) are 60° (0 \AA^{-1}), 55° (0.10 \AA^{-1}), 50° (0.21 \AA^{-1}), and 45° (0.34 \AA^{-1}). The energy loss region below 20 meV is scaled by a factor as indicated. The inset shows the wide range spectrum at $E_p = 7.0$ eV and $\theta_i = \theta_e = 60^\circ$. The energy resolution is 3 meV.

was measured by using an Alumel-Chromel thermocouple attached to the sample holder. After introduced into the chamber, the sample was annealed up to 1300 K, the desorption temperature of hydrogen, and a clean surface was obtained.

For EELS measurements, primary energies (E_p) of 4–19 eV, incidence angles (θ_i) of 60° – 70° , and emission angles (θ_e) of 35° – 70° with respect to the surface normal are used. Typical energy resolution is 3 meV. The phonon dispersion curves are measured along the high-symmetry $\bar{\Gamma}\bar{J}$ and $\bar{\Gamma}\bar{J}'$ directions of the SBZ [Fig. 1(b)] by rotating the energy analyzer around the axis that is perpendicular to the incidence plane of the electron beam. Since the (2×1) and (1×2) domains coexist on the sample surface, the dispersions along both directions are obtained by the measurements along either direction. The wave vector parallel to the surface, Q_{\parallel} , is calculated by $Q_{\parallel} = 0.5123 \sqrt{E_p} (\sin \theta_i - \sin \theta_e) \text{ \AA}^{-1}$. All the EELS measurements are made at 90 K.

Figure 2 shows EELS spectra of the C(001)(2×1) surface as a function of Q_{\parallel} with $E_p = 17.0$ eV and $\theta_i = 60^\circ$. The inset shows a wide range spectrum of C(001)(2×1) with $E_p = 7.0$ eV and $\theta_i = \theta_e = 60^\circ$. The wide-range spectrum

shows no loss due to the C-H stretch mode at ~ 360 meV,^{2,9} ensuring that the surface hydrogen completely desorbs. It is noted that the losses in the 210–320 meV range are ascribed to overtones and combination bands of the fundamental modes. Losses are observed at 92, 119, 126, 135, 146, 154, 164, 172, and 181 meV. The most intense peak at 92 meV shows asymmetric shape with the shoulder on the lower-energy side. Small losses appear at 36 and 68 meV in the off-specular directions.

Our results resemble the previous reports^{7,8} with several loss peaks newly resolved. The intense 92-meV loss is the same as observed in the previous study by Hossain *et al.*,⁷ which was assigned to the bouncing mode of the C-C dimer along the surface normal. They observed additional losses at 123, 135, 147, and 165 meV in the specular direction with $E_p = 6.8$ eV.⁷ They assigned the 123- and 135-meV losses to excitations of transverse optical modes at the W and X points in the bulk Brillouin zone, respectively. The 147-meV loss was assigned as the dimer rocking mode and/or longitudinal mode at X and the 165 meV loss as the dimer twisting mode and/or optical mode at Γ . A recent study by Kinsky *et al.*⁸ showed similar features with the intense peak at 93 meV and small losses ranging from 122 to 180 meV.

It is found that the intensities of the 92-, 119-, and 126-meV peaks decrease significantly in the off-specular directions, indicating the dominant contribution of the dipole scattering to these losses. On the diamond surface, however, it cannot be straightforwardly concluded that these modes are polarized perpendicular to the surface.⁹ This rule is applicable to metallic substrates where the conduction electrons can efficiently screen the dynamic dipole moment induced by the vibrational excitation.¹⁰ However, the dominant contribution of dipole scattering to these modes indicates that the vibrations are derived from the nearby surface, because the bulk modes of the diamond are known to be dipole (infrared) inactive. Note that the surface vibrations below 165 meV on C(001)(2×1) are in resonance with the bulk phonon band,¹¹ and thus, we cannot strictly differentiate the surface and bulk modes in this region.

Theoretical calculations were made using a linear-response scheme to the *ab initio* pseudopotential method¹² applied to a repeated slab geometry. The supercell contained 32 ions located in a slab of 16 atomic layers and a vacuum region equivalent of five atomic layers. Single-particle wave functions were expanded in a plane-wave basis set up to the kinetic energy cutoff of 40 Ryd. The electron-ion interaction was treated by a norm-conserving pseudopotential,¹³ and electron-electron interactions were treated within the local density approximation.¹⁴ The calculations predict 17 surface phonon modes at the $\bar{\Gamma}$ point of the SBZ. The calculated energies and the corresponding displacement patterns are compiled in Fig. 3. The surface dimer belongs to the C_{2v} point group, and thus, the surface phonon modes are classified according to their symmetry species as shown in Fig. 3. Because we measure the spectra on the double-domain C(001)(2×1)-H along the $\bar{\Gamma}\bar{J}$ and $\bar{\Gamma}\bar{J}'$ directions, the normal modes of a_1 , b_1 , and b_2 symmetries can be observed, whereas those of a_2 symmetry are forbidden

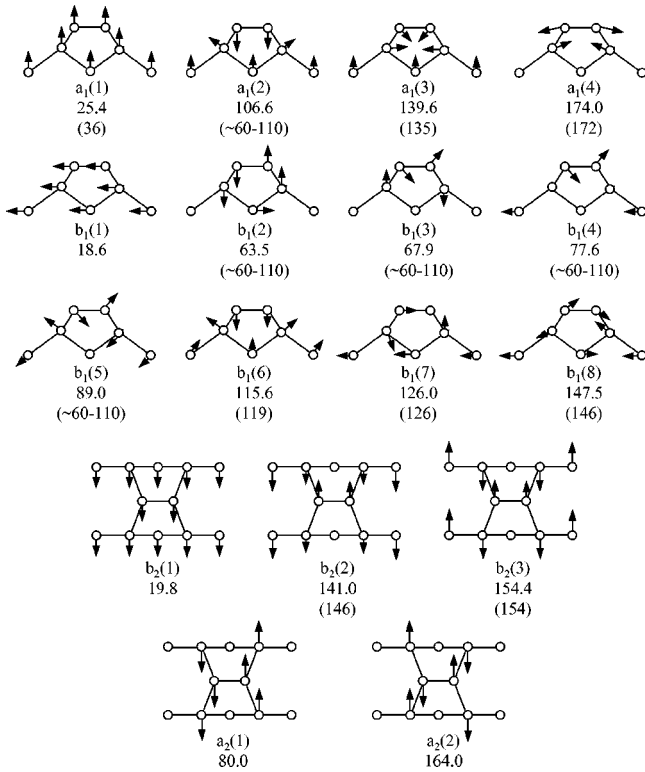


FIG. 3. The displacement patterns of the calculated normal modes at the $\bar{\Gamma}$ point, to which the observed loss peaks are assigned. The normal modes are represented by the symmetry species of the C_{2v} point group. The individual calculated energies are shown with the experimentally observed energies in the brackets in a unit of meV. The a_1 , b_1 , and b_2 modes are observable by EELS.

according to the selection rule for the impact scattering of EELS.¹⁰

The losses are assigned to the calculated phonon modes. The most intense loss at 92 meV and its shoulder dominate EELS spectra in the region of ~ 60 –110 meV. We believe there are several phonon modes which contribute in this region. Judging from the calculated energies, the loss at 92 meV and its shoulder are tentatively assigned to the mixing of $b_1(2)$, $b_1(3)$, $b_1(4)$, $b_1(5)$, and $a_1(2)$ modes, whose energies are in the region of ~ 60 –110 meV. The losses at 119, 126, 135, 146, and 154 meV are assigned as $b_1(6)$, $b_1(7)$, $a_1(3)$, $b_1(8)$ [and perhaps $b_2(2)$], and $b_2(3)$, respectively. The 164-meV loss is attributed to the bulk optical phonon at the $\bar{\Gamma}$ point,¹¹ instead of the symmetry-forbidden $a_2(2)$ mode. Since the losses in the energy region below 165 meV are in resonance with the bulk phonon bands, contributions from the bulk diamond cannot be neglected. The losses at 119 and 126 meV can possibly be contributed from the bulk phonons—namely, the transverse optical (TO) mode at W . The losses at 135 and 146 meV may be attributed to TO mode at X and longitudinal mode at X , respectively.¹¹ The 172- and 181-meV losses lie outside the bulk phonon bands, and we assign the former to the $a_1(4)$ mode, which is calculated to be 174.0 meV (the “stretching” mode). The 181-meV loss is the surface mode but cannot be assigned to any calculated mode. Thus, we tentatively attribute the 181-meV loss to the surface defect species. The 36-meV loss may be assigned to the $a_1(1)$ mode.

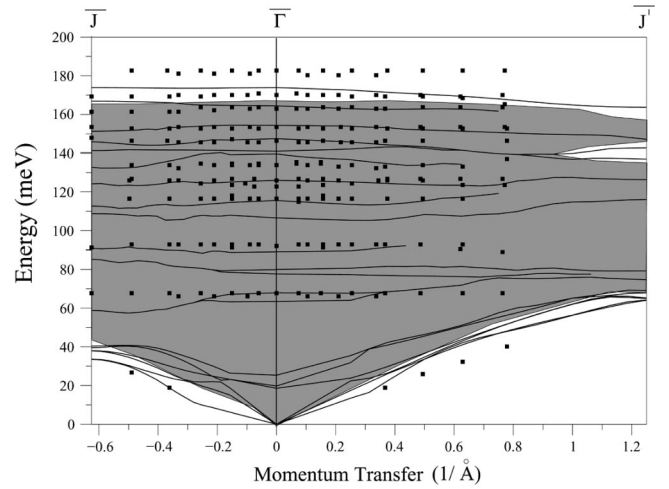


FIG. 4. Measured surface phonon dispersion along the high-symmetry $\bar{\Gamma}\bar{J}$ and $\bar{\Gamma}\bar{J}'$ directions of the C(001)(2×1) surface is shown by solid squares as a function of Q_{\parallel} . Because our sample contains both the (1×2) and (2×1) domains, the data in the two directions are superimposed in the EELS spectra. Thus, we plot the same data in both directions. Due to the experimental limit, only the data for Q_{\parallel} below 0.8 \AA^{-1} are obtained. The calculated results are shown by solid curves. The dark area represents the projected phonon density of states for bulk diamond.

The dispersion of the losses is measured as a function of Q_{\parallel} and shown by solid squares in Fig. 4. We measure the spectra at $E_p = 4$ –19 eV, $\theta_i = 60^\circ$ – 70° , and $\theta_e = 35^\circ$ – 70° . Since the dispersions along the two directions overlap in our experiments, the same data are plotted in both directions. Except for the low-energy Rayleigh mode, all modes show small dispersions of at most 4 meV, which agree well with the previous experimental study.⁸ At E_p higher than 20 eV, the loss intensities significantly attenuate, and thus, dispersion measurements are possible only below $Q_{\parallel} = 0.8 \text{ \AA}^{-1}$. Also shown are the theoretical surface phonon dispersions (solid curves). The experimental results are in resonance with the projected density of states of bulk phonons, represented by the dark area. The theory predicts flat dispersions for almost all losses, which are consistent with the present experimental results.

The dispersion of the loss peaks reflects the dynamical coupling of the vibrations along the surface. The almost-flat features of the losses indicate a nearly localized character of the vibrations along the surface, which is supported by the present theoretical results (see solid curves of Fig. 4). This is in contrast to previous theoretical studies,^{4,6} which suggested that the dynamic coupling between adjacent dimers gives rise to significant energy dispersions of the vibrational modes. For example, the dimer rocking mode was predicted to show an energy difference of 76 meV (Ref. 4) or 82 meV (Ref. 6) between the in-phase ($\bar{\Gamma}$ point) and out-of-phase motions.

In summary, we have investigated the vibrational modes for the diamond C(001)(2×1) surface by means of EELS combined with first-principles theoretical calculations. The zone-center vibrational modes are observed at 36, 68, 92,

119, 126, 135, 146, 154, 164, and 172 meV for the clean C(001)(2×1) surface. Mode assignments of the losses are made by a comparison with the theoretical calculations and bulk phonon measurements. The experimental results agree well with the theoretical predictions not only for the energies of surface phonon modes but also dispersion characteristics.

The losses exhibit little dispersion except for the Rayleigh mode.

This work was supported in part by a Grant-in-Aid from the Ministry of Education, Culture, Sports, Science and Technology (Japan).

-
- ¹W. Kress and F.W. de Wette, *Surface Phonons* (Springer, Berlin, 1991).
- ²S.T. Lee and G. Apai, *Phys. Rev. B* **48**, 2684 (1993).
- ³T. Aizawa, T. Ando, K. Yamamoto, M. Kamo, and Y. Sato, *Diamond Relat. Mater.* **4**, 600 (1995).
- ⁴D.R. Alfonso, D.A. Drabold, and S.E. Ulloa, *Phys. Rev. B* **51**, 1989 (1995).
- ⁵D.R. Alfonso, D.A. Drabold, and S.E. Ulloa, *Phys. Rev. B* **51**, 14669 (1995).
- ⁶T. Frauenheim, T. Köhler, M. Sternberg, D. Porezag, and M.R. Pederson, *Thin Solid Films* **272**, 314 (1996).
- ⁷M.Z. Hossain, T. Kubo, T. Aruga, N. Takagi, T. Tsuno, N. Fujimori, and M. Nishijima, *Jpn. J. Appl. Phys., Part 1* **38**, 6659 (1999).
- ⁸J. Kinsky, R. Graupner, M. Stammer, and L. Ley, *Diamond Relat. Mater.* **11**, 365 (2002).
- ⁹B.D. Thoms and J.E. Butler, *Surf. Sci.* **328**, 291 (1995).
- ¹⁰H. Ibach and D.L. Mills, *Electron Energy Loss Spectroscopy and Surface Vibrations* (Academic Press, New York, 1982).
- ¹¹J.L. Warren, J.L. Yarnell, G. Dolling, and R.A. Cowley, *Phys. Rev.* **158**, 805 (1967).
- ¹²S. Baroni, S. de Gironcoli, A. Dal. Corso, and P. Giannozzi, *Rev. Mod. Phys.* **73**, 515 (2001).
- ¹³R. Stumpf, X. Gonge, and M. Scheffler, *A List of Separable, Norm-conserving, Ab-initio Pseudopotentials* (Fritz-Haber-Institut, Berlin, 1990).
- ¹⁴D.M. Ceperley and B.J. Alder, *Phys. Rev. Lett.* **45**, 566 (1980).